Equivalence of cell survival data for radiation dose and thermal dose in ablative treatments: analysis applied to essential tremor thalamotomy by focused ultrasound and gamma knife

D. Schlesinger[1,3], M. Lee[2], G. ter Haar[4], B. Sela[2], M. Eames[2], J Snell[2], N. Kassell[2,3], J. Sheehan[1,3], J. Larner[1] and J.-F. Aubry[1,5]

1 Department of Radiation Oncology, University of Virginia, Charlottesville, VA

2 Focused Ultrasound Surgery Foundation, Charlottesville, VA

3 Department of Neurosurgery, University of Virginia, Charlottesville, VA

4 Division of Radiotherapy and Imaging, The Institute of Cancer Research:Royal Marsden Hospital, Sutton, Surrey, UK

5 Institut Langevin Ondes et Images, ESPCI ParisTech, CNRS 7587, UMRS 979 INSERM, Paris, France

Running title: Thermal dose and radiation dose comparison

Corresponding Author's address:
jean-francois.aubry@espci.fr

Phone: +33 1 80 96 30 40
Fax: +33 1 80 96 33 55

Declaration of interest : Neal Kassell is an InSightec shareholder.

Summary:

Thermal dose and absorbed radiation dose have been extensively investigated separately over the last decades. The combined effects of heat and ionizing radiation, such as thermal radiosensitization, have also been reported, but the individual modalities have not been compared with each other. In this paper, we propose a comparison of thermal and radiation dose by going back to basics and comparing the cell survival ratios.

Abstract:

Thermal dose and absorbed radiation dose have historically been difficult to compare because different biological mechanisms are at work. Thermal dose denatures proteins and the radiation dose causes DNA damage in order to achieve ablation. The purpose of this paper is to use the proportion of cell survival as a potential common unit by which to measure the biological effect of each procedure.

Survival curves for both thermal and radiation doses have been extracted from previously published data for three different cell types. Fits of these curves were used to convert both thermal and radiation dose into the same quantified biological effect: fraction of surviving cells. They have also been used to generate and compare survival profiles from the only indication for which clinical data are available for both focused ultrasound (FUS) thermal ablation and radiation ablation: essential tremor thalamotomy.

All cell types could be fitted with coefficients of determination greater than 0.992. As an illustration, survival profiles of clinical thalamotomies performed by radiosurgery and FUS are plotted on a same graph for the same metric: fraction of surviving cells.

FUS and Gamma Knife have the potential to be used in combination to deliver a more effective treatment (for example FUS may be used to debulk the main tumor mass, and radiation to treat the surrounding tumor bed). In this case, a model which compares thermal and radiation treatments is valuable in order to adjust the dose between the two.

Key words: ultrasound, thermal dose, radiation dose, damage index, High intensity focused ultrasound

I. Introduction

Therapies involving the use of ionizing radiation and/or thermal energy have a long history in the treatment of disease, including cancer. Evidence from an Egyptian papyryus suggests that as early as 3500 years ago heat was applied in an attempt to treat breast cancer(1, 2). Therapy involving radiation had to wait until the discovery of X-rays in 1895, however within several years of this discovery, radiation therapy based on radionuclides and low-energy X-ray generating equipment was used for the treatment of cancer. (3) More recently there have been parallel developments in the use of heat and ionizing radiation for both diffuse and focal disease, as well as attempts to combine the benefit of the two modalities. A number of techniques have been developed to allow the focal destruction of malignant tissue in humans, including ablation by radiofrequency (4), microwaves(5-12), lasers(13), magnetic nanoparticles(14, 15), and high-intensity focused ultrasound(16-18). Recent advancements in the focal treatment of cancer using ionizing radiation include the development of stereotractic radiosurgery (SRS)(19), stereotactic body radiotherapy (SBRT)(20-22), and intraoperative radiotherapy (IORT) (23, 24).

From an early date and continuing to the present, investigation of the synergies between heat and ionizing radiation have been a natural avenue for research including the basic biology of hyperthermia(25), the most effective sequencing of heating and radiation(26, 27) , biological interactions between heat and radiation(28), and determination of thermal enhancement ratios and predictors of response(28-30). Significant evidence in the form of several randomized control trials exists to demonstrate that hyperthermia followed by radiation can significantly improve outcomes in head and neck cancer(31, 32), malignant melanoma(33), breast cancer (34), glioblastoma multiforme(35), pelvic tumors(36), cervical carcinoma(37), superficial tumors(38), cervical cancer(39), non-small-cell lung cancer(40), rectal cancer(41), among

others(2, 42). The recent progress in focal ablative therapies such as HIFU and SRS/SBRT may also benefit from combined approaches. However, direct comparison of absorbed dose in ionizing radiation and thermal dose for heating have historically been difficult because of the widely different physical and biological mechanisms in play(1).

In this work, we compare thermal and ionizing radiation modalities in terms of biological damage to tissue by using equivalent historical in-vitro cell survival data. By doing so, we aim to create a method for translation between measures of thermal and radiation dose. Essential tremor thalamotomy is currently the only indication for which quantitative clinical data are available for both radiation and FUS treatments. In order to illustrate this approach, we thus took into account the beam shaping capabilities of the stereotactic radiosurgery (SRS) and FUS devices available for treatment of essential tremor, in order to allow more direct comparison between FUS and SRS treatments. Our approach could facilitate dosimetry planning in the setting of combined radiosurgery and FUS.

A. Biological effect of ionizing radiation and definition of radiation dose

Photon-based ionizing radiation (X-rays and γ-rays) are indirectly ionizing; they deposit energy in tissue in a two-step process. In the first step, photolectric and Compton interactions between photons and atoms in tissue result in the transfer of energy to fast electrons ejected from the target atoms. In a second step, atoms in the targeted tissue are ionized as these fast electrons undergo Coulomb interactions with other atoms in the targeted tissue, transferring a fraction of their energy during each interaction(43). In traditional radiobiology theory, the biological target of ionizing radition is damage to DNA. In a minority of cases (~33%), DNA is directly ionized, leading to strand breaks. In the majority of cases (~66%), the ions created in irradiated tissue result in the creation of free radicals (most significantly hydroxyl radicals) which subsequently react with and create strand breaks in DNA. The ultimate biological effect of the DNA damage

is mitotic death of the cells in the irradiated tissue(1). At higher, ablative doses there may additional biological mechanisms at play as well, including microvascular damage(44). Radiation dose is described in physical terms; the amount of energy absorbed per mass of tissue. This is the definition of "absorbed dose", and is most commonly assigned units of Gray (Gy), where 1 Gy = 1 J/kg of energy absorbed in tissue (43). The amount of biological damage caused can be related directly to the physical quantity of absorbed dose, and this has become the standard method of prescribing the appropriate amount of radiation to be delivered in any given therapeutic setting.

B. Biological effect of thermal energy and definition of thermal dose

The response of cells to thermal insult at sub-ablative temperatures (such as temperatures employed in traditional hyperthermia) can be quite complex, involving the development of a combination of thermotolerance, cytotoxicity, and radiosensitization most likely mediated by protein denaturation within cells which increases proportionately to the thermal damage. Lower level of protein denaturation can trigger protective mechanisms such as increased expression of heat shock proteins which help to stabilize the cell against further thermal damage. Higher levels of protein denaturation can cause the inactivation of protein synthesis and DNA repair mechanisms resulting in cytotoxity and increased sensitivity to ionizing radiation. (45) When delivered at sufficient power to result in ablation, thermal energy ultimately results in coagulative necrosis(46). As with ionizing radiation, the extent of biological changes in tissue resulting from thermal exposure is correlated with the amount of energy absorbed in tissue. However, for thermal energy, it is the temperature to which the tissue is raised, and the duration of the heating that seem to play the predominent biological role. Sapareto and Dewey have defined a 'thermal isoeffective dose' (47). This has units of cumulative equivalent minutes at 43°C (CEM 43°C), and allows conversion of any temperature/time (T/t) combination to the

equivalent time for which the reference temperature of 43°C must be applied to obtain the same level of thermal damage:

$$CEM_{43} = \int_0^t R^{43-T(t)} dt$$

$$R = \begin{cases} 0.25 & if\ T < 43°C \end{cases}$$

The definition of the thermal isoeffective dose formalizes the idea that two different temperatures applied over different time intervals can have the same biological effect in a given tissue.

C. Cell survival curves

Traditionally, the most common method for assessing cell survival in thermo- and radiobiology uses survival curves. The principle of survival curve analysis is the same, irrespective of the source of cell damage. The curve depicts the relationship between the damage to which a cell has been subjected and the cell's subsequent ability to divide to form a colony. . For the studies considered here, *in vitro* assays have been used as the source data. The development of survival curves involve plating a known number of cells (determined using a standard counting method) out into tissue culture dishes following exposure to heat or ionizing radiation, and analyzing their response at a later time point. The surviving fraction is calculated by normalizing the number of cells or colonies seen in treated samples to that seen in controls. This is then plotted on a logarithmic scale against the thermal or radiation dose delivered.(1) A minimum colony size (usually 50 cells) is used as a cutoff for minimal critical mass of cells to survive as a colony. It should be noted, that while this type of assay is frequently assumed to measure individual cell survival directly, the reduction in number after treatment may also be due in part to cells going into a "dormant" state, and not dividing. (1)Typical survival curves are shown in Figure 1 for radiotherapy and thermal doses. For thermal treatments, the cells were subjected to

a variety of temperatures as shown in the figure legend. However, when both temperature and time are taken into account by calculating thermal dose in CEM, the data fall along a common curve.

II. Materials and methods

A. Literature Review

An extensive review of the literature was conducted to identify studies reporting cell survival for thermal exposure, with the goal of identifying cell subtypes for which there were matching published reports on cell survival for ionizing radiation. Basically a literature review for both thermal and radiation cell survival was performed and then data were cross referenced. The literature review was conduced using Cornell University's online library during June and July of 2013. Key words used in this literature review included: cell survival, radiation treatment, thermal treatment, thermal dose, radiation dose, tissue damage, and hyperthermia. Some exclusion criteria included: articles not written in English, studies that only used thermal and radiation treatment in combination, and studies that did not measure cell survival. Table 1 lists the publications selected for thermal and ionizing radiation modalities. The list is not exhaustive and the literature search was stopped when three different cell-types were found for which survival data was available: Chinese hamster ovary cells (CHO), Chinese hamster lung cells (CHL), and human glioblastoma tumor cells will thus be used in the rest of the article to illustrate our approach.

B. Data Extraction and Cell Survival Modeling

Each point of the survival data, as displayed in the reports selected for thermal and ionizing radiation experiments, was manually transferred into Matlab version R2013a (Mathworks, Inc., Natick, MA) for each cell type: Chinese Hamster Ovary (CHO), Chinese Hamster Lung (CHL),

and Human Glioblastoma Astrocytoma (GBA). The radiation dose survival profiles for each of the 3 cell types were modeled using the Universal Survival Curve (USC) developed by Park, et al(48). The USC is one of several derivatives of the linear quadratic model that attempt to take into account low and high doses survival regimes (44, 49-53):

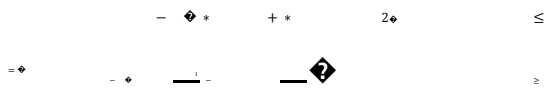

where S is the cell survival, defined as the ratio between the remaining number of undamaged cells at time t indicated by N(t) to the number of undamaged cells N(0) present prior to the start of the treatment, D_r is the radiation dose in Gray, n is the number of fractionations, and α (units of $\log_e$ of the cells killed per Gy) and β (units $\log_e$ of cells killed per Gy^2) are constants that describe the linear and quadratic portions of the curve, respectively. D_T is the transition dose, where the curve changes from using the low dose model to the high dose. D_o is a measure of the slope of the linear portion of the curve at high doses and D_q is the x-intercept of the survival line valid for ≤ . β and D_T are calculated from the parameters α , D_o, and D_q to ensure continuity and differentiability at D_T (48):

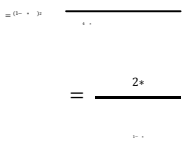

In traditional radiobiology, the α and β terms above are also often represented in ratio form (the α/β ratio, units of Gy), which is the dose at which the linear and quadratic components are equal. Tumors and tissue which show an early response to radiation damage tend to have a large α/β ratio, while tissue which shows a late response to radiation damage have a small α/β ratio)(1, 53, 54). Thermal dose survival data were fitted with a linear-quadratic equation for all 3 cell types (55, 56)):

where S is the cell survival, D_t is the thermal dose in equivalent minutes, and a and b are constants.

Damage index Ω is widely used for RF and laser ablation. It is the logarithm of the ratio between the number of undamaged cells N(0) present prior to the start of the treatment to the remaining number of undamaged cells at time t indicated by N(t) (57):

$$\Omega = \ln \frac{N(0)}{N(t)} = \ln \frac{1}{S}$$

Ω can thus be expressed as a function of the thermal dose with the same fit coefficients a and b calculated above:

$$\Omega = a + b^2$$

D. Evaluation of clinical treatment spot sizes

For sake of illustration, clinical data from both radiation surgery and thermal ablation have been processed. The only indication which the authors could get access to data sets for both is essential tremor. Thalamotomy data for both FUS and SRS were thus analyzed for predicted cell survival. The clinical data used for analysis is anonymized data from a pilot study for essential tremor patients conducted at the University of Virginia(58) under oversight and approval of the university's institutional review board (IRB). The anonymized Gamma Knife SRS dose distributions for the 3 cases used in the analysis have been determined by the IRB to be not subject to IRB review.

1. Focused Ultrasound

The clinical FUS study consisted of 15 patients with essential tremor whose condition did not improve with medication. The patients were treated with MR-guided FUS, targeting the ventral intermediate (VIM) nucleus of the thalamus. A series of low-power sonications were delivered

to the intended target to validate the geometric accuracy of the setup.

Temperature maps were recorded during treatment using MR thermometry(59). In this study, the temperature for each voxel was read from the raw data files for each timepoint of the sonication and used to calculate the thermal dose. The thermal dose profile was determined by normalizing the data to the maximum thermal dose in the volume of interest.

Using the calculated thermal profiles and the cell survival-thermal dose relationship for all cell lines (CHO, CHL and GBA), cell survival was calculated for each voxel in the region of interest.

2. Gamma Knife Radiosurgery

The clinical radiosurgery data is derived from treatment plans for 3 radiosurgical thalamotomies performed on the Gamma Knife at University of Virginia for individuals with essential tremor that have failed to improve with other treatments and are unwilling, or unable, to undergo an invasive procedure. Radiosurgical thalamotomy was achieved using the Leksell Gamma Knife to deliver a maximum dose of 130-140Gy with a 4mm isocenter to the VIM nucleus on the opposite side of the brain from the more severe tremor. The technique employed at the University of Virginia is similar to techniques published in the literature. (60)

SRS dose distributions were created using the Gamma Knife treatment planning software (Leksell GammaPlan versions 8.0 - 10.1, Elekta AB, Stockholm). The resulting dose distributions were exported in anonymized DICOM-RT format. The radiotherapy dose profiles in x and y directions were averaged and then normalized to the maximum administered dose and converted to a percentage. Using the cell survival-radiotherapy dose relationship for CHO, CHL and GBA, the fraction of cells surviving was determined as a function of distance.

III. Results

1. Cell survival fitting

The resulting cell survival curves, extracted from previous studies, (61-66) are shown in Figure 2 for radiotherapy and thermal dose.

Results are summarized in Table 2. The α/β values for the radiation treatment on the 3 types of cells are close to previously published values.(54, 67, 68). The linear quadratic fit of the curves resulted in an average coefficient of determination of R^2=0.995 , a maximum of 0.998, and a minimum of 0.992. All R^2 values are displayed in Table 2. In order to achieve a cell survival fraction of 10^{-5} (i.e. a survival of 0.001%), a radiotherapy dose of 17Gy must be applied to CHO cells, 20.5Gy to CHL cells, and 14Gy to GBA cells. To achieve the same percentage of surviving cells a thermal dose of 148.5CEM must be administered to the targeted CHO cells, 178CEM to CHL cells, and 249.5CEM to GBA cells.

2. Estimated cell survival from clinical MRgFUS and Gamma Knife essential tremor treatments

The dose profiles from the clinical essential tremor data for FUS and SRS are shown in Figure 3A, normalized to the point of maximum delivered dose (3160 CEM for thermal and 130 Gy for SRS). 10% of the maximum dose is delivered to cells at 1.6mm for thermal dose and at 6.9mm for radiotherapy exposures. As seen in the simulated profiles, the thermal dose profile drop off is sharp and by 3mm the dose is at zero. For the radiotherapy dose, the drop off is much more gradual and reaches an average of 4% of the maximum dose at 11 mm.

The corresponding simulated cell survival curves for the essential tremor clinical data are displayed in Figure 3B. As an example, for GBA cells, the survival curve for the radiotherapy dose clinical data reaches a level of 90% at 28.9mm and 99.5% at 27.78mm. For the thermal dose, 90% survival occurs at a distance of 3.71mm and reaches 99.5% survival at a distance of 6.5mm. The survival curve for radiotherapy dose drops off more gradually than the thermal dose survival curve (Figure 3A).

IV. Discussion

Potential clinical applications of FUS overlap significantly with SRS. FUS is being considered as a substitute modality for radiotherapy for indications such as essential tremor, neuropathic pain, and others. However, the techniques do not need to compete. A more common scenario may be to use FUS in combination with radiotherapy, especially in the treatment of malignant disease. In this setting, FUS may be used to debulk the main tumor mass, allowing for significant and immediate symptomatic relief. This may be followed by radiation to the surrounding tumor bed with the goal of reducing local failure and regional recurrences. Investigators are also looking at the reverse approach, where the tumor and the surrounding tumor bed are first irradiated to damage the ability of the cells to reproduce. This is then followed by FUS to debulk the main tumor.

In either situation, a method of quantifying the biological damage inflicted on both normal and diseased tissue from both modalities, like the one introduced in this paper, would be valuable, and in particular for areas of tissue receiving sub-lethal doses from either modality on its own.

Historically, creating a direct comparison between thermal dose and radiation dose has been considered impractical (1). This is in part because the concept of absorbed dose for ionizing radiation describes the physics of the situation; i.e. the energy absorbed by a mass of tissue from exposure to ionizing radiation (43). Conversely, the formulation of the thermal iso-effective dose, is based on empirically observed effects in heated cells.

However, SRS (19) and FUS surgery (16, 69) attempt to achieve a similar biological effect: the ablation of a volume of tissue. SRS, especially when delivered in a single fraction, delivers a dose to tissue that can be considered “ablative” in the sense that the expected surviving fraction of cells is low (70). Likewise, FUS achieves ablation of a desired region of tissue by heating to a thermal isoeffect dose known to cause coagulative necrosis with a similarly negligible surviving cell fraction (71, 72). A threshold for damage of 240CEM was determined in vivo in dog prostate(73) and in muscle(74) and

corresponds to the threshold used in most clinical systems(75). Normalization to a similar biological endpoint makes feasible a direct comparison of radiation dose and thermal isoeffect. The threshold thermal or radiation dose required to "just" achieve ablation gives us a sort of "calibration" point in the spectrum of biological damage at which to equate the two dose formulations.

Equating the dose fomulations might benefit the planning of combination therapies which take advantage of the synergistic effect of radiotherapy and thermal ablation. Compared to RF ablation alone, RF ablation combined with radiation therapy has been shown to increase the ablation volume in rat tumors(76) and improve survival(77), has shown a low rate of complications in patients with unresectable lung cancer(78-80) and has increased the relapse-free survival rate in prostate adenocarcinoma (81). This pioneering work could be revisited in an optimal way by taking advantage of the non invasive and conformal treatment capabilities of focused ultrasound and external beam therapy for inducing thermal and radiation effects with 3D planning based on the cell survival formulation proposed here.

The thermal energy resulting in cytotoxicity drops off faster than for radiation therapy (Fig. 3). In part, this is related to the physics and technical details of the devices. Gamma Knife, used as a platform for the radiosurgery dose distibutions in our study, achieves a steep dose profile through the application of a large number (192 in the Perfexion model Gamma Knife used in this study) cross-firing beams that are collimated so they intersect with high precision at a focal point. A single irradiation location, or "isocenter" creates an approximately spherical dose distribution. Irradiation of irregularly shaped targets is achieved by using multiple isocenters and collimator settings at different positions. The dose falloff on a Gamma Knife is fundamentally dependent on the attenuation of each beam (which is at 60Co energy), the penumbra of each beam, and the total number of beams, and the isodose level in the distribution placed at the treatment margin of the target(82). The sharper spatial distribution falloff of the thermal dose is linked to the size of each individual heated region (focal spot) and thus to the ultrasonic transducer geometry, and the frequency used. This is not unexpected as thermal conduction

is a very inefficient method of heating tissue(83): thermal conduction is an inherent limitation for large treatment volumes with focused ultrasound as the focal spot is small. The whole volume needs to be treated spot by spot. Nevertheless, limited diffusion can also be seen as an advantage as it contributes to a sharper boundary and a better control of energy deposition.

A. Limitations of this study

The intent of this paper was to explore the potential utility of equating thermal dose and radiation dose effects using cell survival as a common unit of measurement. As there is limited data collected with the intent of making such a direct comparison, there are assumptions that impact the uncertainties in the analysis including the in-vitro cell survival data used in the study, the the accuracy of survival models at ablative doses, and simplification of the possible complexities of the joint biological effects of thermal energy and ionizing radiation.

Limitations of in-vitro cell survival data in this study

Perhaps the most significant limitation of our experiment is that in-vitro studies do not represent clinical reality. By design, in-vitro experiments use cells grown under carefully controlled conditions. The in-vivo situation is obviously much more complex; for example our models do not take into account the heat sink effect of the surrounding tissue vasculature (84), cell-cycle differences (85), or tissue inhomogenities which can distort thermal and radiation dose (86-88). Stochastic models have shown that time-temperature history, tumor geometry, tumor perfusion, and uniformity of heating are all likely to affect cell survival rates(89). Nor do in-vitro models account for immunological effects, inflammatory effects, chemokines, or cytokines that are present in-vivo. (90, 91)In addition, the cell lines used to create the thermal dose and radiation dose survival curves in this paper do not correspond with the cell types (i.e. normal brain tissue) irradiated during a FUS thalamotomy or radiosurgery thalamotomy. This was because of the non-existence of published data for our chosen clinical example. The mismatch between in-vitro cell lines and the cells found in human brain tissue creates

uncertainties on the specific parameters determined for our model fit. As in-vitro and in-vivo cell survival data is accrued for thermal and radiation doses over a larger range of cell-types, the method presented in this paper can be refined to include better parameter estimates.

Limitations of survival models at ablative doses

Another limitation to our approach is that the mathematical models used for thermal and radiation dose derive from in-vitro cell survival data acquired at sub-ablative doses. Both the thermal dose and ionizing radiation cell survival models have been shown to have weaknesses at high, single-fraction doses. Ideally, experiments should be conducted on the same types of cells, with the same cell survival assay and for SRS-like doses. Multiple models for thermal damage and radiation damage could also be employed to better represent the likely uncertainty in the calculations(92). This is beyond the scope of the present paper.

Simplifying assumptions regarding the joint biological effects of thermal energy and ionizing radiation

A simplifying assumption of the study is that thermal dose and radiation dose may be treated independently. In practice, there is likely some degree of interaction between the two. For instance, hyperthermia studies have demonstrated in-vitro that the achievable radiosensitization caused by heating is dependent on the sequence and time interval between heating and irradiation. While data remains inconclusive, there is a consensus that simultaneous heating and irradiation would maximize the dose enhancement effect due to heat, and as the interval between heat and radiation increases (regardless of sequence) the degree of enhancement decreases(26). Radiosensitization may also be enhanced through heating by preferentially killing chronically hypoxic tissue as is often found in the center of malignant tumors as they grow. These hypoxic regions tend to be radioresistant, and it is unclear how using heat to destroy these regions would effect the overall sensitivity profile to a joint treatment. A related effect is that heating can cause increased perfusion to targeted tissue, helping to reoxygenate (and thus radiosensitize) hypoxic areas of tissue(93, 94).

This study attempts to relate thermal dose and radiation dose at a very low "ablative" level of cell kill, perhaps avoiding some of the complexities of the interactions between the biology of thermal and radiation insults. The thermal dose profiles presented in the results include a thin region of sub-lethally heated tissue. This tissue likely benefits from some of the radiosensitization that has been demonstrated from these earlier hyperthermia results, and this is not accounted for in our model. However further investigation will be required to understand what, if any, clinical significance these sub-lethally heated regions would have on the ultimate outcome of a joint thermal/radiation treatment and how it might affect thermal or radiation dose prescriptions.

B. Other Limitations of the work

Finally, different tissue and organ types have differential sensitivity to both ionizing and thermal dose. This is also not modeled in the current approach, however it is inherent in the in-vitro cell data used in the study. Differential response to ionizing radiation is partly related to the length of the cell-cycle of a given cell type, as lethal DNA damage is manifested during mitosis. Cells with short lifespans tend to show early reaction to radiation insult. Slower-dividing cells tend to show later reactions.(1) The primary mechanism of thermal cell death is a combination of protein denaturation and coagulative necrosis. This could reasonably be assumed to be similar across all cell lines. The differences then may be due to alternative mechanism of cell death such as disruption of intracellular signal transduction and cell motility(42, 95, 96)

V. Conclusion:

Radiation- and thermal- based treatments are difficult to compare because of the differences in the physics of the energy deposition and the resulting biological effects . The work presented in this paper is a first attempt at creating a method of equating thermal and radiation doses for ablative treatments by considering "ablation" as a common biological endpoint. It was shown how radiation dose and thermal

dose could both be expressed in terms of percentage of surviving cells, and thus be compared with the same quantitative effect on tissues. Much work remains to be done in order to validate the regression equations and dose models against both in-vitro and in-vivo targets of different heterogeneous tissues.

IV. Figures and Tables

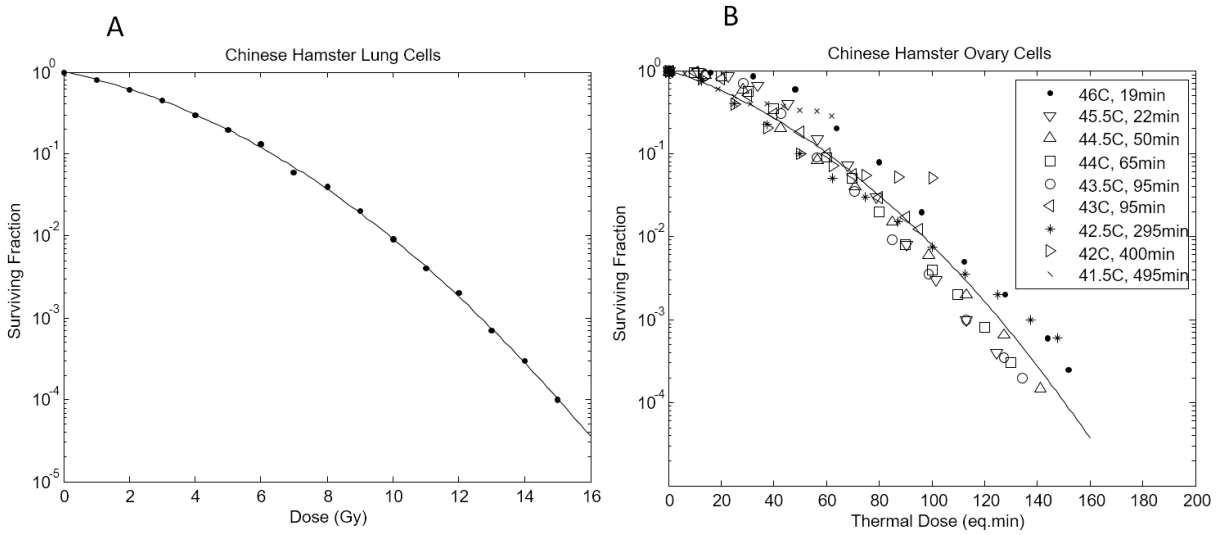

FIGURE 1. Figure 1: An example of a survival curve for radiotherapy exposure (A), extracted from (97), and for heated cells (B), extracted from previously published results (98), with thermal isoeffective dose calculated from the combination of heating duration and temperature

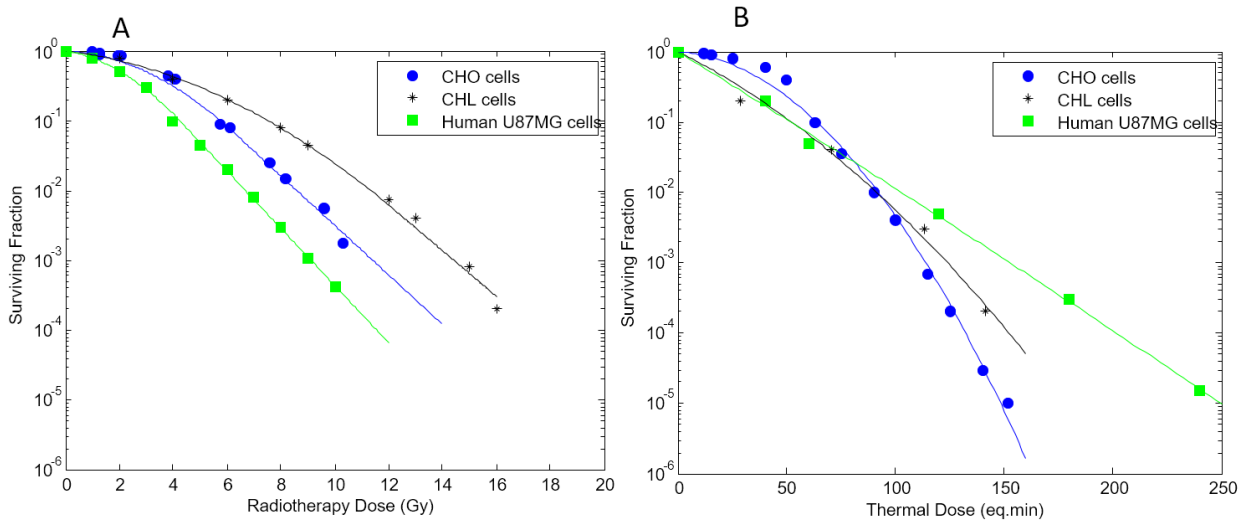

FIGURE 2. Fraction of cells surviving as a function of the radiation (A) or thermal (B) dose for (●) CHO, (♦) CHL, and (■) GBA. Data have been extracted from previously published results: (CHO),(61) (CHL),(62) (GBA)(65) (A) and (CHO),(63) (CHL),(66) (GBA)(64) (B).

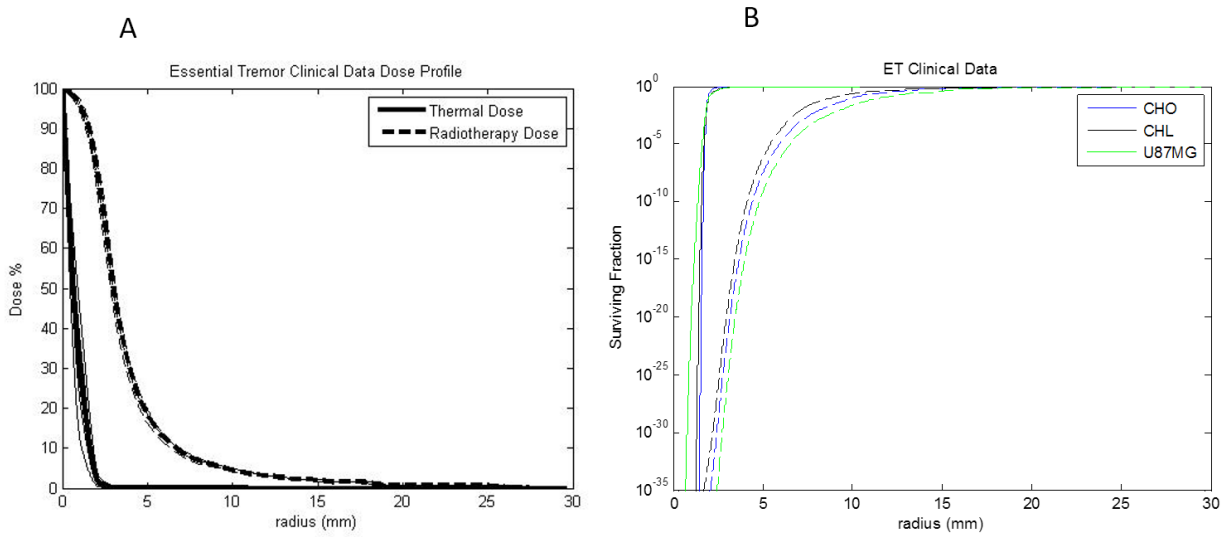

FIGURE 3. Average dose profiles (A) and corresponding survival curves (B) for essential tremor clinical data. The average profiles amongst patients are shown in four directions from the center and the average is highlighted in bold (A) . Survival curves for essential tremor clinical data for FUS (solid) and SRS (dashed) are plotted for each cell type available.

Reference Article	Type of Tissue Investigated		Treatment Modality	Dose Range
Sensitivity of Human Cells to Mild Hyperthermia [24]	Human Glioblastoma Tumor Cells	U87MG	Heat	0-240 CEM
Thermal Dose Determination in Cancer Therapy [21]	Chinese Hamster Ovary		Heat	0-150 CEM
Cellular Effects of Hyperthermia: Relevance to the minimum dose for thermal damage[25]	Chinese Hamster Lung	V79	Heat	0-150 CEM
Arrhenius Relationships from the Molecule and Cell to the Clinic[26]	Chinese Hamster Ovary		Heat	0-150 CEM
Basic Principles of thermal dosimetry and thermal threshold for tissue damage from hyperthermia [27]	Chinese Hamster Ovary		Heat	0-180 CEM
A Transient Thermotolerant Survival Response Produced by Single Thermal Doses in HeLa Cells [28]	HeLa		Heat	0-480 CEM
Differential Effect of Hyperthermia on Murine Bone Marrow Normal Colony-forming Units and AKR and L1210 Leukemia Stem Cells [29]	Leukemia Cells	L1210, AKR	Heat	0-60 CEM
A Comparison of Cell Killing by Heat and/or X Rays in Chinese Hamster V79 Cells, Friend Erythroleukemia Mouse Cells, and Human Thymocyte MOLT-4 [30]	Chinese Hamster Lung	V79	Radiation	0-16 Gy
Cellular Responses to Combinations of Hyperthermia and Radiation [31]	Chinese Hamster Ovary		Radiation	0-11 Gy
Cross-Resistance to Ionizing Radiation in a Murine Leukemic Cell Line Resistant to cis-Dichlorodiammineplatinum(II): Role of Ku Autoantigen [32]	Leukemia Cells	L1210	Radiation	0-10 Gy
Effect of Hyperthermia on the Radiation Response of two Mammalian Cell Lines [33]	Chinese Hamster Ovary , mouse mammary sarcoma	HA-1, EMT-6	Radiation	0-12 Gy
Effects of propranolol in combination with radiation on apoptosis and survival of gastric cancer cells in vitro [34]	Human gastric adenocarcinoma cells	BGC-823, SGC-7901	Radiation	0-10 Gy
Enhancement of Radiation Damage in Cellular DNA Following Unifilar Substitution with Iododeoxyuridine [35]	Chinese Hamster Lung	V79	Radiation	0-16 Gy
Hyperthermia Radiosensitization in Human Glioma Cells Comparison of Recovery of Polymerase Activity, Survival, and Potentially Lethal Damage Repair [36]	Human Glioblastoma Tumor Cells	U87MG	Radiation	0-12 Gy
Influence of Hyperthermia on Gamma-Ray-Induced Mutation in V79 Cells [37]	Chinese Hamster Lung	V79	Radiation	0-12 Gy
Interaction of Hyperthermia and Radiation in CHO Cells: Recovery Kinetics [38]	Chinese Hamster Ovary		Radiation	0-12 Gy
Long duration mild temperature hyperthermia and brachytherapy [39]	Human Normal fibroblasts, Human radiation resistant melanoma cells, Human Ovarian Carcinoma cells	AG1522, SkMe13, A2780	Radiation	0-10 Gy

Moderate Hyperthermia and Low Dose Irradiation [22]	Chinese Hamster Lung	V79	Radiation	0-14 Gy
Radiosensitivity and Capacity to Recover from Radiation Induced Damage in Pimonisazol-Unlabeled Intratumor Quiescent Cells Depend on p53 Status [40]	Human head and neck squamous carcinoma cells	SAS	Radiation	0-14 Gy
Recovery of Sublethal Radiation Damage and is inhibition by Hyperthermia in normal and transformed mouse cells [41]	Chinese Hamster Lung	V79	Radiation	0-14 Gy
The p65 subunit of nuclear factor-κB is a molecular target for radiation sensitization of human squamous carcinoma cells [42]	Human head and neck squamous carcinoma cells	SCC-35, d6, d12	Radiation	0-11 Gy
Thermal radiosensitization in Chinese hamster and mouse C3H 10T 1/2 cells. The thermotolerance effect [40]	Chinese Hamster Lung, mouse embryo	V79, C3H	Radiation	0-14 Gy
Thermal Sensitivity and Radiosensitization in V79 Cells after BrdUrd or IdUrd Incorporation [43]	Chinese Hamster Lung	V79	Radiation	0-16 Gy
Thermally Enhanced Radioresponse of Cultured Chinese Hamster Cells: Inhibition of Repair of Sublethal Damage and Enhancement of Lethal Damage [44]	Chinese hamster fibroblasts	V79	Radiation	0-11 Gy
Thermal sensitivity and radiosensitization in Chinese hamster V79 cells exposed to 2-aminopurine or 6-thioguanine [45]	Chinese Hamster Lung	V79	Radiation	0-14 Gy

TABLE 1. Review of papers reporting survival of cells exposed to thermal rise or ionizing radiations, matched for cell subtype and dose range.

USC fit (radiation dose)	**α (1/Gy)**	**β ($1/Gy^2$)**	**α/β (Gy)**	**D_q (Gy)**	**D_o (Gy)**	**D_T (Gy)**	**R^2**
CHO	0.043	0.062	0.69	2.93	1.23	6.19	0.993
CHL	0.11	0.026	4.12	5.23	1.33	12.22	0.995
GBA	0.14	0.094	1.53	1.81	1.06	4.28	0.996
Exponential fit (thermal dose)	**a (1/CEM)**		**b ($1/CEM^2$)**		**a/b (CEM)**		**R^2**
CHO	0.0047		0.00049		9.6		0.994
CHL	0.035		0.00017		210		0.992
GBA	0.044		9.1e-6		4800		0.998

TABLE 2. Parameters for the Universal Survival Curve (USC) for radiation therapy doses and linear quadratic exponential fit for thermal doses.

References

1. Hall EJ, Giaccia AJ. Radiobiology For The Radiologist: Lippincott Williams&Wilki; 2006.
2. Horsman MR, Overgaard J. Hyperthermia: a potent enhancer of radiotherapy. Clin Oncol-Uk. 2007 Aug;19(6):418-26. PubMed PMID: WOS:000248780400005. English.
3. Lederman M. The early history of radiotherapy: 1895-1939. International journal of radiation oncology, biology, physics. 1981;7(5):639-48.
4. Haemmerich D. Biophysics of radiofrequency ablation. Critical reviews in biomedical engineering. 2010;38(1):53.
5. Carrafiello G, Ierardi AM, Fontana F, Petrillo M, Floridi C, Lucchina N, et al. Microwave ablation of pancreatic head cancer: safety and efficacy. Journal of vascular and interventional radiology : JVIR. 2013 Oct;24(10):1513-20. PubMed PMID: 24070507.
6. Chen JC, Moriarty JA, Derbyshire JA, Peters RD, Trachtenberg J, Bell SD, et al. Prostate cancer: MR imaging and thermometry during microwave thermal ablation-initial experience. Radiology. 2000 Jan;214(1):290-7. PubMed PMID: 10644139.
7. Healey TT, Dupuy DE. Microwave ablation for lung cancer. Medicine and health, Rhode Island. 2012 Feb;95(2):52-3. PubMed PMID: 22474876.
8. Kuang M, Lu MD, Xie XY, Xu HX, Mo LQ, Liu GJ, et al. Liver cancer: increased microwave delivery to ablation zone with cooled-shaft antenna--experimental and clinical studies. Radiology. 2007 Mar;242(3):914-24. PubMed PMID: 17229876.
9. Skinner MG, Iizuka MN, Kolios MC, Sherar MD. A theoretical comparison of energy sources - microwave, ultrasound and laser - for interstitial thermal therapy. Physics in Medicine and Biology. 1998;43(12):3535.
10. Vargas HI, Dooley WC, Gardner RA, Gonzalez KD, Venegas R, Heywang-Kobrunner SH, et al. Focused microwave phased array thermotherapy for ablation of early-stage breast cancer: results of thermal dose escalation. Annals of surgical oncology. 2004 Feb;11(2):139-46. PubMed PMID: 14761916.
11. Yoshitani S, Hayashi K, Kuroda M, Tanaka Y, Hasegawa T, Saito H, et al. [Results of local ablation therapy for liver metastases from colorectal cancer using radiofrequency ablation and microwave coagulation therapy (RFA/MCT)]. Gan to kagaku ryoho Cancer & chemotherapy. 2005 Oct;32(11):1666-9. PubMed PMID: 16315903.
12. Zhang X, Chen B, Hu S, Wang L, Wang K, Wachtel MS, et al. Microwave ablation with cooled-tip electrode for liver cancer: an analysis of 160 cases. Hepato-gastroenterology. 2008 Nov-Dec;55(88):2184-7. PubMed PMID: 19260502.
13. Ali MA, Carroll KT, Rennert RC, Hamelin T, Chang L, Lemkuil BP, et al. Stereotactic laser ablation as treatment for brain metastases that recur after stereotactic radiosurgery: a multiinstitutional experience. Neurosurgical focus. 2016 Oct;41(4):E11. PubMed PMID: 27690654.
14. Latorre M, Rinaldi C. Applications of magnetic nanoparticles in medicine: magnetic fluid hyperthermia. Puerto Rico health sciences journal. 2009 Sep;28(3):227-38. PubMed PMID: 19715115.
15. Tseng HY, Lee GB, Lee CY, Shih YH, Lin XZ. Localised heating of tumours utilising injectable magnetic nanoparticles for hyperthermia cancer therapy. IET nanobiotechnology / IET. 2009 Jun;3(2):46-54. PubMed PMID: 19485552.
16. Hynynen K, Darkazanli A, Unger E, Schenk J. MRI-guided non-invasive ultrasound surgery. Medical Physics. 1993;20:107-15.
17. Ebbini ES, Ter Haar G. Ultrasound-guided therapeutic focused ultrasound: current status and future directions. International Journal of Hyperthermia. 2015;31(2):77-89.
18. Maloney E, Hwang JH. Emerging HIFU applications in cancer therapy. International Journal of Hyperthermia. 2015;31(3):302-9.
19. Leksell L. The stereotaxic method and radiosurgery of the brain. Acta Chir Scand. 1951 Dec

13;102(4):316-9. PubMed PMID: 14914373. Epub 1951/12/13. eng.
20. Blomgren H, Lax I, Naslund I, Svanstrom R. Stereotactic high dose fraction radiation therapy of extracranial tumors using an accelerator. Clinical experience of the first thirty-one patients. Acta oncologica. 1995;34(6):861-70. PubMed PMID: 7576756.
21. Papiez L, Timmerman R, DesRosiers C, Randall M. Extracranial stereotactic radioablation: physical principles. Acta oncologica. 2003;42(8):882-94. PubMed PMID: 14968949.
22. Timmerman R, Papiez L, McGarry R, Likes L, DesRosiers C, Frost S, et al. Extracranial stereotactic radioablation: results of a phase I study in medically inoperable stage I non-small cell lung cancer. Chest. 2003 Nov;124(5):1946-55. PubMed PMID: 14605072.
23. Dieterich S, Ford E, Pavord D, Zeng J. Practical Radiation Oncology Physics: A Companion to Gunderson and Tepper's Clinical Radiation Oncology: Elsevier - Health Sciences Division; 2015.
24. Gunderson LL, Willett CG, Calvo FA, Harrison LB. Intraoperative Irradiation: Techniques and Results: Humana Press; 2011.
25. Dewey WC, Holahan EV. Hyperthermia--basic biology. Progress in experimental tumor research. 1984;28:198-219. PubMed PMID: 6484202.
26. Overgaard J. Influence of sequence and interval on the biological response to combined hyperthermia and radiation. National Cancer Institute monograph. 1982 Jun;61:325-32. PubMed PMID: 7177183.
27. Kosterev VV, Kramer-Ageev EA, Mazokhin VN, van Rhoon GC, Crezee J. Development of a novel method to enhance the therapeutic effect on tumours by simultaneous action of radiation and heating. International Journal of Hyperthermia. 2015;31(4):443-52.
28. Gillette EL. Clinical use of thermal enhancement and therapeutic gain for hyperthermia combined with radiation or drugs. Cancer Res. 1984 Oct;44(10 Suppl):4836s-41s. PubMed PMID: 6467236.
29. Dewhirst MW, Sim DA. The utility of thermal dose as a predictor of tumor and normal tissue responses to combined radiation and hyperthermia. Cancer Res. 1984 Oct;44(10 Suppl):4772s-80s. PubMed PMID: 6380715.
30. Overgaard J. Formula to estimate the thermal enhancement ratio of a single simultaneous hyperthermia and radiation treatment. Acta radiologica Oncology. 1984;23(2-3):135-9. PubMed PMID: 6331081.
31. Valdagni R, Amichetti M. Report of long-term follow-up in a randomized trial comparing radiation therapy and radiation therapy plus hyperthermia to metastatic lymph nodes in stage IV head and neck patients. Int J Radiat Oncol Biol Phys. 1994 Jan 1;28(1):163-9. PubMed PMID: 8270437.
32. Huilgol NG, Gupta S, Sridhar CR. Hyperthermia with radiation in the treatment of locally advanced head and neck cancer: a report of randomized trial. Journal of cancer research and therapeutics. 2010 Oct-Dec;6(4):492-6. PubMed PMID: 21358087.
33. Overgaard J, Gonzalez Gonzalez D, Hulshof MC, Arcangeli G, Dahl O, Mella O, et al. Hyperthermia as an adjuvant to radiation therapy of recurrent or metastatic malignant melanoma. A multicentre randomized trial by the European Society for Hyperthermic Oncology. Int J Hyperthermia. 1996 Jan-Feb;12(1):3-20. PubMed PMID: 8676005.
34. Vernon CC, Hand JW, Field SB, Machin D, Whaley JB, van der Zee J, et al. Radiotherapy with or without hyperthermia in the treatment of superficial localized breast cancer: results from five randomized controlled trials. International Collaborative Hyperthermia Group. Int J Radiat Oncol Biol Phys. 1996 Jul 1;35(4):731-44. PubMed PMID: 8690639.
35. Sneed PK, Stauffer PR, McDermott MW, Diederich CJ, Lamborn KR, Prados MD, et al. Survival benefit of hyperthermia in a prospective randomized trial of brachytherapy boost +/- hyperthermia for glioblastoma multiforme. Int J Radiat Oncol Biol Phys. 1998 Jan 15;40(2):287-95. PubMed PMID: 9457811.
36. van der Zee J, González D, van Rhoon GC, van Dijk JD, van Putten WL, Hart AA. Comparison

of radiotherapy alone with radiotherapy plus hyperthermia in locally advanced pelvic tumours: a prospective, randomised, multicentre trial. The Lancet. 2000;355(9210):1119-25.
37. Harima Y, Nagata K, Harima K, Ostapenko VV, Tanaka Y, Sawada S. A randomized clinical trial of radiation therapy versus thermoradiotherapy in stage IIIB cervical carcinoma. Int J Hyperthermia. 2001 Mar-Apr;17(2):97-105. PubMed PMID: 11252361.
38. Jones EL, Oleson JR, Prosnitz LR, Samulski TV, Vujaskovic Z, Yu D, et al. Randomized trial of hyperthermia and radiation for superficial tumors. Journal of clinical oncology : official journal of the American Society of Clinical Oncology. 2005 May 1;23(13):3079-85. PubMed PMID: 15860867.
39. Vasanthan A, Mitsumori M, Park JH, Zhi-Fan Z, Yu-Bin Z, Oliynychenko P, et al. Regional hyperthermia combined with radiotherapy for uterine cervical cancers: a multi-institutional prospective randomized trial of the international atomic energy agency. Int J Radiat Oncol Biol Phys. 2005 Jan 1;61(1):145-53. PubMed PMID: 15629605.
40. Mitsumori M, Zeng ZF, Oliynychenko P, Park JH, Choi IB, Tatsuzaki H, et al. Regional hyperthermia combined with radiotherapy for locally advanced non-small cell lung cancers: a multi-institutional prospective randomized trial of the International Atomic Energy Agency. International journal of clinical oncology. 2007 Jun;12(3):192-8. PubMed PMID: 17566842.
41. Schroeder C, Gani C, Lamprecht U, von Weyhern CH, Weinmann M, Bamberg M, et al. Pathological complete response and sphincter-sparing surgery after neoadjuvant radiochemotherapy with regional hyperthermia for locally advanced rectal cancer compared with radiochemotherapy alone. Int J Hyperthermia. 2012;28(8):707-14. PubMed PMID: 23006132.
42. Mallory M, Gogineni E, Jones GC, Greer L, Simone CB, 2nd. Therapeutic hyperthermia: The old, the new, and the upcoming. Critical reviews in oncology/hematology. 2016 Jan;97:56-64. PubMed PMID: 26315383.
43. Khan FM. The Physics of Radiation Therapy: Wolters Kluwer Health; 2012.
44. Kirkpatrick JP, Meyer JJ, Marks LB. The linear-quadratic model is inappropriate to model high dose per fraction effects in radiosurgery. Seminars in radiation oncology. 2008;18:240-3. PubMed PMID: 18725110.
45. Lepock JR. How do cells respond to their thermal environment? International journal of hyperthermia : the official journal of European Society for Hyperthermic Oncology, North American Hyperthermia Group. 2005 Dec;21(8):681-7. PubMed PMID: 16338849.
46. Mouratidis PX, Rivens I, ter Haar G. A study of thermal dose-induced autophagy, apoptosis and necroptosis in colon cancer cells. International Journal of Hyperthermia. 2015;31(5):476-88.
47. Sapareto SA, Dewey WC. Thermal dose determination in cancer therapy. Int J Radiat Oncol Biol Phys. 1984 Jun;10(6):787-800. PubMed PMID: 6547421. Epub 1984/06/01. eng.
48. Park C, Papiez L, Zhang S, Story M, Timmerman RD. Universal survival curve and single fraction equivalent dose: useful tools in understanding potency of ablative radiotherapy. International journal of radiation oncology, biology, physics. 2008;70:847-52. PubMed PMID: 18262098.
49. Kavanagh BD, Newman F. Toward a Unified Survival Curve: In Regard to Park< i> et al.</i>(< i> Int J Radiat Oncol Biol Phys</i> 2008; 70: 847–852) and Krueger< i> et al.</i>(< i> Int J Radiat Oncol Biol Phys</i> 2007; 69: 1262–1271). International Journal of Radiation Oncology* Biology* Physics. 2008;71(3):958-9.
50. Wang JZ, Huang Z, Lo SS, Yuh WT, Mayr NA. A generalized linear-quadratic model for radiosurgery, stereotactic body radiation therapy, and high–dose rate brachytherapy. Science translational medicine. 2010;2(39):39ra48-39ra48.
51. Hanin LG, Zaider M. Cell-survival probability at large doses: an alternative to the linear-quadratic model. Physics in medicine and biology. 2010;55:4687-702. PubMed PMID: 20671352.
52. Astrahan M. Some implications of linear-quadratic-linear radiation dose-response with regard to hypofractionation. Medical Physics. 2008;35:4161.
53. Guerrero M, Li XA. Extending the linear–quadratic model for large fraction doses pertinent to

stereotactic radiotherapy. Physics in Medicine and Biology. 2004;49:4825-35.
54. Garcia LM, Wilkins DE, Raaphorst GP. Alpha/beta ratio: A dose range dependence study. International journal of radiation oncology, biology, physics. 2007;67(2):587.
55. McDannold N, Zhang Y-Z, Power C, Jolesz F, Vykhodtseva N. Nonthermal ablation with microbubble-enhanced focused ultrasound close to the optic tract without affecting nerve function: Laboratory investigation. Journal of neurosurgery. 2013;119(5):1208-20.
56. Carlson DJ, Stewart RD, Semenenko VA, Sandison GA. Combined use of Monte Carlo DNA damage simulations and deterministic repair models to examine putative mechanisms of cell killing. 2009.
57. Viglianti BL, Dewhirst MW, Abraham JP, Gorman JM, Sparrow EM. Rationalization of thermal injury quantification methods: application to skin burns. Burns. 2014;40(5):896-902.
58. Elias WJ, Huss D, Voss T, Loomba J, Khaled M, Zadicario E, et al. A Pilot Study of Focused Ultrasound Thalamotomy for Essential Tremor. New England Journal of Medicine. 2013;369(7):640-8. PubMed PMID: 23944301.
59. Rieke V, Butts Pauly K. MR thermometry. Journal of Magnetic Resonance Imaging. 2008;27(2):376-90.
60. Kondziolka D, Ong JG, Lee JY, Moore RY, Flickinger JC, Lunsford LD. Gamma Knife thalamotomy for essential tremor. 2008.
61. Dewey W, Hopwood L, Sapareto S, Gerweck L. Cellular responses to combinations of hyperthermia and radiation. Radiology. 1977;123(2):463-74.
62. Raaphorst GP, Szekely J, Lobreau A, Azzam EI. A comparison of cell killing by heat and/or X rays in Chinese hamster V79 cells, Friend erythroleukemia mouse cells, and human thymocyte MOLT-4 cells. Radiation research. 1983;94(2):340-9.
63. Flentje M, Flentje D, Sapareto SA. Differential effect of hyperthermia on murine bone marrow normal colony-forming units and AKR and L1210 leukemia stem cells. Cancer Res. 1984 May;44(5):1761-6. PubMed PMID: 6713379. Epub 1984/05/01. eng.
64. Armour EP, McEachern D, Wang Z, Corry PM, Martinez A. Sensitivity of human cells to mild hyperthermia. Cancer research. 1993;53(12):2740-4.
65. Raaphorst GP, Feeley MM. Hyperthermia radiosensitization in human glioma cells comparison of recovery of polymerase activity, survival, and potentially lethal damage repair. International Journal of Radiation Oncology, Biology, Physics. 1994;29(1):133-9.
66. Lepock JR. Cellular effects of hyperthermia: relevance to the minimum dose for thermal damage. International journal of hyperthermia. 2003;19(3):252-.
67. Scheenstra AEH, Rossi MMG, Belderbos JSA, Damen EMF, Lebesque JV, Sonke J-J. Alpha/Beta Ratio for Normal Lung Tissue as Estimated From Lung Cancer Patients Treated With Stereotactic Body and Conventionally Fractionated Radiation Therapy. International Journal of Radiation Oncology, Biology, Physics. 2014;88(1):224.
68. Williams MV, Denekamp J, Fowler JF. A review of alpha/beta ratios for experimental tumors: implications for clinical studies of altered fractionation. International journal of radiation oncology, biology, physics. 1985;11(1):87.
69. Hynynen K, Colucci V, Chung A, Jolesz F. Noninvasive arterial occlusion using MRI-guided focused ultrasound. Ultrasound Med Biol. 1996;22(8):1071-7. PubMed PMID: 9004431. Epub 1996/01/01. eng.
70. Abbas G, Schuchert MJ, Pennathur A, Gilbert S, Luketich JD. Ablative treatments for lung tumors: radiofrequency ablation, stereotactic radiosurgery, and microwave ablation. Thorac Surg Clin. 2007 May;17(2):261-71. PubMed PMID: 17626404. Epub 2007/07/14. eng.
71. Dewhirst MW, Lora-Michiels M, Viglianti BL, Dewey WC, Repacholi M. Carcinogenic effects of hyperthermia. Int J Hyperthermia. 2003 May-Jun;19(3):236-51. PubMed PMID: 12745970. Epub 2003/05/15. eng.

72. Fry W, Mosberg W, Barnard J, Fry F. Production of focal destructive lesions in the central nervous system with ultrasound. J Neurosurg. 1954;11:471-8.
73. Yarmolenko PS, Moon EJ, Landon C, Manzoor A, Hochman DW, Viglianti BL, et al. Thresholds for thermal damage to normal tissues: an update. International Journal of Hyperthermia. 2011;27(4):320-43.
74. Dewey W. Arrhenius relationships from the molecule and cell to the clinic. International journal of hyperthermia. 1994;10(4):457-83.
75. Foley JL, Eames M, Snell J, Hananel A, Kassell N, Aubry J-F. Image-guided focused ultrasound: state of the technology and the challenges that lie ahead. Imaging in Medicine. 2013 2013/08/01;5(4):357-70.
76. Solazzo S, Mertyna P, Peddi H, Ahmed M, Horkan C, Nahum Goldberg S. RF ablation with adjuvant therapy: comparison of external beam radiation and liposomal doxorubicin on ablation efficacy in an animal tumor model. International Journal of Hyperthermia. 2008;24(7):560-7.
77. Horkan C, Dalal K, Coderre JA, Kiger JL, Dupuy DE, Signoretti S, et al. Reduced Tumor Growth with Combined Radiofrequency Ablation and Radiation Therapy in a Rat Breast Tumor Model 1. Radiology. 2005;235(1):81-8.
78. Grieco CA, Simon CJ, Mayo-Smith WW, DiPetrillo TA, Ready NE, Dupuy DE. Percutaneous image-guided thermal ablation and radiation therapy: outcomes of combined treatment for 41 patients with inoperable stage I/II non–small-cell lung cancer. Journal of vascular and interventional radiology. 2006;17(7):1117-24.
79. Chan MD, Dupuy DE, Mayo-Smith WW, Ng T, DiPetrillo TA. Combined radiofrequency ablation and high–dose rate brachytherapy for early-stage non–small-cell lung cancer. Brachytherapy. 2011;10(3):253-9.
80. Imada H, Nomoto S, Tomimatsu A, Kosaka K, Kusano S, Ostapenko V, et al. Local control of nonsmall cell lung cancer by radiotherapy combined with high power hyperthermia using an 8 MHz RF capacitive heating device. Jpn J Hyperthermic Oncol. 1999;15:19-24.
81. Anscher MS, Samulski TV, Dodge R, Prosnitz LR, Dewhirst MW. Combined external beam irradiation and external regional hyperthermia for locally advanced adenocarcinoma of the prostate. International Journal of Radiation Oncology* Biology* Physics. 1997;37(5):1059-65.
82. Lindquist C, Paddick I. The Leksell Gamma Knife Perfexion and comparisons with its predecessors. Neurosurgery. 2007 Sep;61(3 Suppl):130-40; discussion 40-1. PubMed PMID: 17876243.
83. Livraghi T, Mueller PR, Silverman SG, van Sonnenberg E, McMullen W, Solbiati L. Tumor ablation: principles and practice: Springer Science & Business Media; 2008.
84. Lagendijk J, Schellekens M, Schipper J, Van der Linden P. A three-dimensional description of heating patterns in vascularised tissues during hyperthermic treatment. Physics in medicine and biology. 1984;29(5):495.
85. Barranco SC, Romsdahl MM, Humphrey RM. The Radiation Response of Human Malignant Melanoma Cells Grown in Vitro. Cancer research. 1971 June 1, 1971;31(6):830-3.
86. Aubry JF, Tanter M, Pernot M, Thomas JL, Fink M. Experimental demonstration of noninvasive transskull adaptive focusing based on prior computed tomography scans. J Acoust Soc Am. 2003 Jan;113(1):84-93. PubMed PMID: 12558249. Epub 2003/02/01. eng.
87. Clement G, Hynynen K. A non-invasive method for focusing ultrasound through the human skull. Physics in Medicine and Biology. 2002;47:1219-36.
88. Moskvin V, Timmerman R Fau - DesRosiers C, DesRosiers C Fau - Randall M, Randall M Fau - DesRosiers P, DesRosiers P Fau - Dittmer P, Dittmer P Fau - Papiez L, et al. Monte carlo simulation of the Leksell Gamma Knife: II. Effects of heterogeneous versus homogeneous media for stereotactic radiosurgery. 20041208 DCOM- 20050323(0031-9155 (Print)). eng.
89. Rosner GL, Clegg ST, Prescott DM, Dewhirst MW. Estimation of cell survival in tumours

heated to nonuniform temperature distributions. Int J Hyperthermia. 1996 Mar-Apr;12(2):223-39. PubMed PMID: 8926391.
90. Hong ZY, Song KH, Yoon JH, Cho J, Story MD. An experimental model-based exploration of cytokines in ablative radiation-induced lung injury in vivo and in vitro. Lung. 2015 Jun;193(3):409-19. PubMed PMID: 25749666.
91. Kahn J, Tofilon PJ, Camphausen K. Preclinical models in radiation oncology. Radiation oncology. 2012 Dec 27;7:223. PubMed PMID: 23270380. Pubmed Central PMCID: 3549821.
92. Pearce JA. Comparative analysis of mathematical models of cell death and thermal damage processes. Int J Hyperthermia. 2013 Jun;29(4):262-80. PubMed PMID: 23738695.
93. Griffin RJ, Dings RP, Jamshidi-Parsian A, Song CW. Mild temperature hyperthermia and radiation therapy: role of tumour vascular thermotolerance and relevant physiological factors. Int J Hyperthermia. 2010;26(3):256-63. PubMed PMID: 20210610. Pubmed Central PMCID: 2909325.
94. Song CW, Shakil A, Griffin RJ, Okajima K. Improvement of tumor oxygenation status by mild temperature hyperthermia alone or in combination with carbogen. Seminars in oncology. 1997 Dec;24(6):626-32. PubMed PMID: 9422259.
95. Liang P, MacRae TH. Molecular chaperones and the cytoskeleton. Journal of cell science. 1997 Jul;110 (Pt 13):1431-40. PubMed PMID: 9224761.
96. Pratt WB, Silverstein AM, Galigniana MD. A model for the cytoplasmic trafficking of signalling proteins involving the hsp90-binding immunophilins and p50cdc37. Cellular signalling. 1999 Dec;11(12):839-51. PubMed PMID: 10659992.
97. Ling CC, Robinson E. Moderate hyperthermia and low dose rate irradiation. Radiation research. 1988;114(2):379-84.
98. Sapareto SA, Hopwood LE, Dewey WC, Raju MR, Gray JW. Effects of hyperthermia on survival and progression of Chinese hamster ovary cells. Cancer research. 1978;38(2):393.